9-1-2012

The 1.17 Day Orbit of the Double-Degenerate (da+dq) nltt 16249

S. Vennes
Czech Academy of Sciences

A. Kawka
Czech Academy of Sciences

S. J. O'Toole
Australian Astronomical Observatory

J. R. Thorstensen
Dartmouth College

The Astrophysical Journal Letters, 756:L5 (4pp), 2012 September 1 doi:10.1088/2041-8205/756/1/L5

THE 1.17 DAY ORBIT OF THE DOUBLE-DEGENERATE (DA+DQ) NLTT 16249*

S. Vennes[1,4], A. Kawka[1,4], S. J. O'Toole[2], and J. R. Thorstensen[3]
[1] Astronomický ústav, Akademie věd České republiky, Fričova 298, CZ-251 65 Ondřejov, Czech Republic
[2] Australian Astronomical Observatory, P.O. Box 296, 1710 Epping NSW, Australia
[3] Department of Physics and Astronomy, 6127 Wilder Laboratory, Dartmouth College, Hanover, NH 03755-352, USA
Received 2012 June 21; accepted 2012 July 25; published 2012 August 8

ABSTRACT

New spectroscopic observations show that the double-degenerate system NLTT 16249 is in a close orbit ($a = 5.6 \pm 0.3\,R_\odot$) with a period of 1.17 days. The total mass of the system is estimated between 1.47 and 2.04 $M_\odot$ but it is not expected to merge within a Hubble timescale ($t_{\rm merge} \approx 10^{11}$ yr). Vennes & Kawka originally identified the system because of the peculiar composite hydrogen (DA class) and molecular (C_2–DQ class and CN) spectra and the new observations establish this system as the first DA plus DQ close double degenerate. Also, the DQ component was the first of its class to show nitrogen dredged up from the core in its atmosphere. The star may be viewed as the first known DQ descendant of the born-again PG1159 stars. Alternatively, the presence of nitrogen may be the result of past interactions and truncated evolution in a close binary system.

Key words: binaries: close – stars: fundamental parameters – white dwarfs

1. INTRODUCTION

The high proper motion star NLTT 16249 is a double-degenerate system showing hydrogen lines and molecular carbon and cyanogen bands in its optical spectrum (Vennes & Kawka 2012). Although large radial velocity variations were noted by Vennes & Kawka (2012), the orbital parameters, period, and separation are yet to be determined. The detection of photospheric nitrogen in the carbon-rich (DQ) component of this system was a first occurrence for this class of objects and, according to the dredge-up scenario commonly applied to DQ white dwarfs (Pelletier et al. 1986; MacDonald et al. 1998), it implied the presence of nitrogen in the white dwarf core. The other component is a hydrogen-rich (DA) white dwarf with a mass above average but with a luminosity similar to that of the DQ white dwarf.

The two characteristics of the system, a nitrogen-enriched DQ component and a likely close orbit, may or may not be related. Althaus et al. (2005) established a clear evolutionary link between born-again stars and a nitrogen/oxygen enrichment in PG1159 stars and their DQ descendents. Members of the PG1159 class have a helium-rich surface with notable enrichment in carbon, nitrogen, and oxygen (Werner et al. 1991; Dreizler & Heber 1998; Werner & Herwig 2006). Althaus et al. (2005) argued that not all DQ stars followed the born-again path because the carbon abundance is lower in some of these objects than would be expected following this evolutionary path. However, the log C/He versus $T_{\rm eff}$ trend established by Dufour et al. (2005) and Koester & Knist (2006) does appear to follow the model predictions of Althaus et al. (2005). Moreover, Dufour et al. (2005) noted two discernible tracks with one at a higher carbon abundance that was attributed to a thinning of the helium layer. Therefore, data and born-again models may be compatible for the bulk of DQ white dwarfs. However, nitrogen is not detected in any DQ stars other than in the DQ in NLTT 16249.

In this Letter, we present convincing evidence that the components of the binary NLTT 16249 are in a close orbit. Our new radial velocity measurements (Section 2) and our original model atmosphere analysis (Vennes & Kawka 2012) help constrain the component properties and offer clues to the origin and evolutionary prospect of the system (Section 3). We summarize and discuss these new results in Section 4.

2. OBSERVATIONS

Vennes & Kawka (2012) described the discovery and initial observations of the double-degenerate NLTT 16249: on UT 2010 March 26, they obtained three low-dispersion spectra using the Ritchey–Chrétien (R-C) spectrograph attached to the 4 m telescope at Kitt Peak National Observatory (KPNO). Next, on UT 2010 November 7, they obtained an echelle spectrum using the X-shooter spectrograph attached to the UT2 at Paranal Observatory.

The apparent radial velocity variations and the composite nature of the original spectra prompted us to obtain a more comprehensive time series. We re-observed NLTT 16249 at Siding Spring Observatory (SSO), KPNO, and the MDM Observatory (on Kitt Peak).

On UT 2011 December 2–3, we obtained a set of spectra with the Wide Field Spectrograph (WiFeS; Dopita et al. 2007) attached to the 2.3 m telescope at SSO. On December 2, we obtained three exposures of 15 minutes each, and on December 3, two exposures of 30 minutes each. We used the B3000 and R7000 gratings which provided spectral ranges of 3200–5900 Å at a resolution $R = \lambda/\Delta\lambda = 3000$, and 5300–7000 Å at $R = 7000$, respectively. We used the RT560 dichroic beam splitter to separate the incoming light into its red and blue components. We maximized the signal-to-noise ratio of each observation by extracting the spectrum from the most significant ($\lesssim$6) traces. Each trace was wavelength and flux calibrated prior to co-addition. The spectra were wavelength calibrated using NeAr arc spectra that were obtained following each observation.

Next, on 2012 January 4–6, we used the 4 m telescope and R-C spectrograph at KPNO. The KPC-24 grating in second order and the T2KA CCD delivered a spectral resolution of ~0.9 Å from 6030 to 6720 Å with the slit width set to 1.″5.

* Based on observations made with ESO telescopes at the La Silla Paranal Observatory under program ID 86.D-0562.
[4] Visiting Astronomer, Kitt Peak National Observatory, National Optical Astronomy Observatory, which is operated by the Association of Universities for Research in Astronomy (AURA) under cooperative agreement with the National Science Foundation.

Table 1
Radial Velocities

HJD (2450000+)	v_{DA} (km s^{-1})	v_{DQ} (km s^{-1})	HJD (2450000+)	v_{DA} (km s^{-1})	v_{DQ} (km s^{-1})	HJD (2450000+)	v_{DA} (km s^{-1})	v_{DQ} (km s^{-1})
5507.83298	152.0	−65.6	5930.90103	−37.5	...	5931.96734	−5.7	...
5898.10485	...	107.1	5930.95874	−9.3	...	5932.60763	181.5	...
5899.19171	−36.9	114.9	5931.63937	82.8	...	5932.67638	155.3	...
5930.64584	7.5	...	5931.69918	62.6	...	5932.80138	88.1	...
5930.71365	−32.9	...	5931.77189	11.7	...	5932.91735	32.4	...
5930.78652	−36.3	...	5931.79347	17.1	...	5932.96735	8.4	...
5930.84654	−24.6	...	5931.90289	−30.7	...	5944.85259	...	100.6

Table 2
Binary Parameters

Parameter	Measurement
Period	$P = 1.1697^{+0.0057}_{-0.0037}$ days
Initial epoch (HJD)	$T_0 = 2455898.34^{-0.15}_{+0.10}$
Semi-amplitude (DA)	$K_{DA} = 104.6 \pm 3.7$ km s^{-1}
Mean velocity (DA)	$\gamma_{DA} = 69.3 \pm 2.8$ km s^{-1}
Semi-amplitude (DQ)	$K_{DQ} = 97.4 \pm 5.1$ km s^{-1}
Mass ratio	$q \equiv M_{DQ}/M_{DA} = 1.1 \pm 0.1$

We sorted the first and second orders using a GG495 filter. We obtained 17 exposures of 30 minutes, each one followed by a comparison arc (HeNeAr).

Finally, on 2012 January 18, we used the MDM 2.4 m Hiltner telescope and modular spectrograph (modspec). A thick 2048^2 CCD gave 1.7 Å pixel^{-1} and ∼3.5 Å resolution from 4460 to 7770 Å, with vignetting toward the ends of the range. We obtained three consecutive exposures (5, 5, and 10 minutes). All spectra were reduced using standard IRAF procedures.

3. ANALYSIS

3.1. Radial Velocities and Period Analysis

The narrow Hα line core proved suitable for precise radial velocity measurements of the DA white dwarf. When available, the sharp edges of the C_2 and CN band heads also offer means to measure relative DQ velocities. Consequently, we measured the DA radial velocity by fitting Gaussian functions to the narrow Hα core (v_{DA} in Table 1). The measurement errors were estimated by varying the location of the continuum when fitting the line core and we noted fluctuations of 2–5 km s^{-1} depending on the signal-to-noise ratio. The centering of the target on the slit is the largest source of systematic errors. These errors were estimated at ∼1/10 of a resolution element or ∼5 km s^{-1} for a resolution $R \approx 7000$. On the other hand, residuals in the wavelength calibration never exceeded 1–2 km s^{-1} and were similar to velocity fluctuations of the O I λλ6300.23, 6363.88 sky lines. Adding systematic and random errors, we conservatively estimated the total error at 10 km s^{-1}.

Next, we re-measured the DQ velocity in the UVB X-shooter spectrum using the C_2 Swan band head at 5162.2 Å and the CN violet band head at 3883.4 Å and listed the average measurement in Table 1. The measurements are consistent with those originally employed by Vennes & Kawka (2012). The MDM and SSO spectra were then cross-correlated with the X-shooter spectrum to extract new DQ velocities (v_{DQ} in Table 1). Consecutive spectroscopic series obtained at SSO or MDM were co-added to maximize the signal-to-noise ratio and decrease the error in velocity measurements. The original KPNO data obtained by Vennes & Kawka (2012) are not included in the present set because of their lower spectral resolution ($R \approx 1000$).

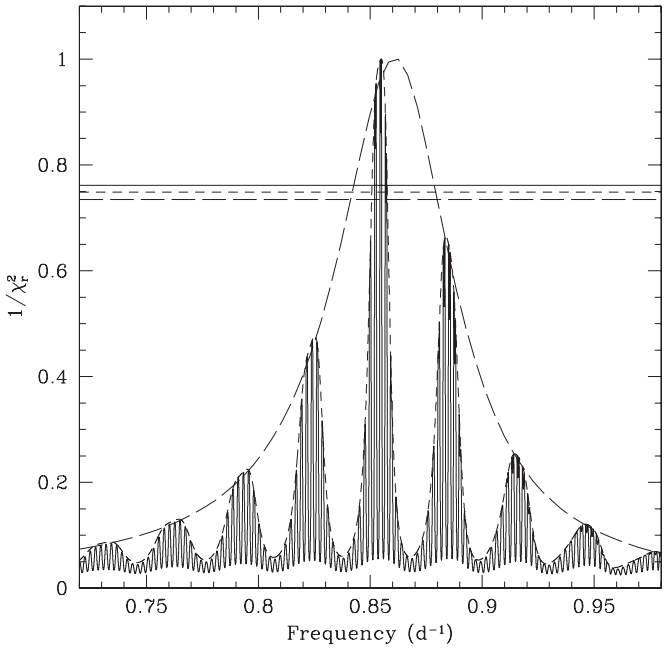

Figure 1. Frequency analysis (inverse of the reduced χ^2_r vs. frequency, $1/P$) of the Hα data (v_{DA}, Table 1) including the KPNO data only (long-dashed line), the KPNO and SSO data (short-dashed line), and the complete data set (X-shooter, KPNO, and SSO; full line). The horizontal lines mark 1σ confidence levels for the corresponding data sets.

Finally, we fitted the sinusoidal function $v = \gamma + K \times \sin(2\pi(t - T_0)/P)$ as a function of time (HJD t) to the DA radial velocity data and determined simultaneously the initial epoch (T_0), period (P), mean velocity (γ), and velocity semi-amplitude (K). We normalized the χ^2 function so that the minimum reduced $\chi^2_{r,\min} \equiv 1$. The 1σ range is then estimated using $\chi^2_{r,1\sigma} = \chi^2_{r,\min} + c/(N-p) = 1 + 4.7/(N-4)$, where N is the number of measurements, $p = 4$ is the number of parameters, and $c = 4.7$ is the appropriate constant for a 1σ error range and four parameters. Figure 1 shows incremental frequency ($1/P$) analyses. The period extracted from the KPNO radial velocity data alone ($N = 17$), $P = 1.161 \pm 0.026$ days, is sufficiently accurate to constrain the DA velocity amplitude and mass function of the DQ companion. Adding SSO measurements to the set ($N = 18$) reduced the period uncertainty and allowed accurate phasing of the DQ velocity measurements as well (Table 2) with a period of $P = 1.1697^{+0.0057}_{-0.0037}$ days.

Adding X-shooter data to the set ($N = 19$) resolved the solution into a triplet with each of the triplet members split

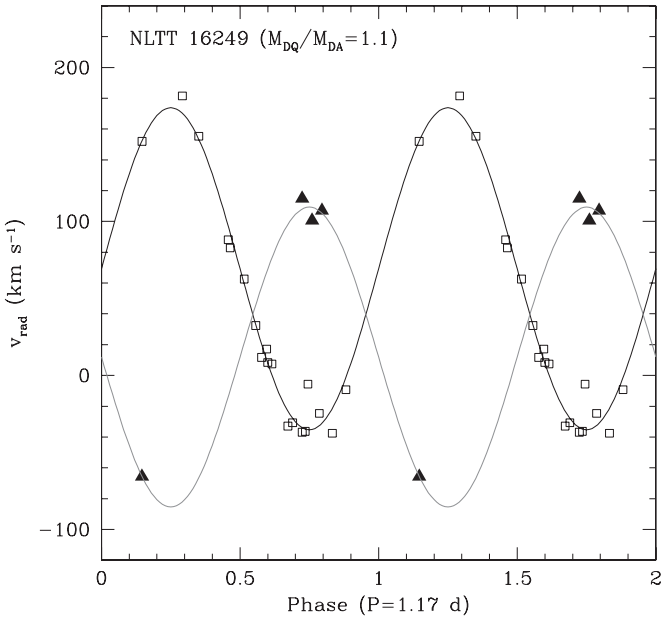

Figure 2. All radial velocity measurements from Table 1 folded on the orbital period: DA white dwarf $v_{\rm DA}$ (open squares) and DQ white dwarf $v_{\rm DQ}$ (full triangles). The velocity amplitudes constrain the mass ratio to nearly unity ($q \equiv M_{\rm DQ}/M_{\rm DA} = 1.1 \pm 0.1$).

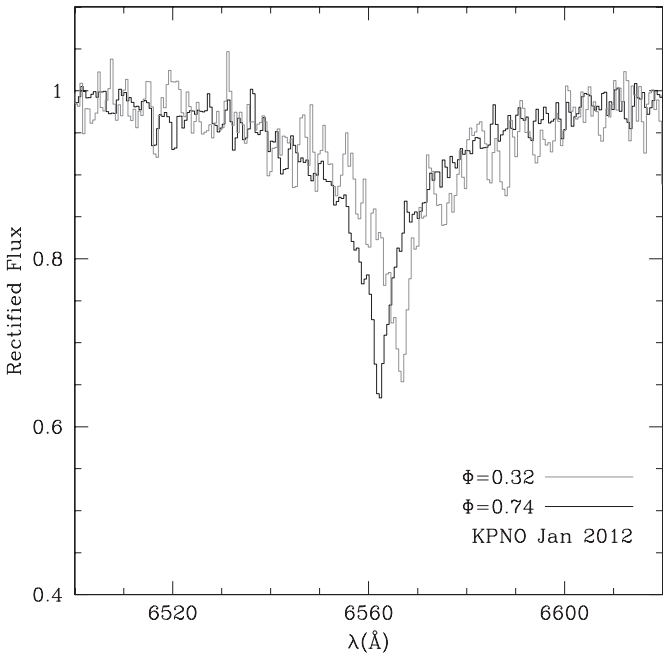

Figure 3. Sets of co-added Hα spectra near quadratures. The Hα line core is shifted by ∼4 Å between the two sets.

into two possible periods. Focusing on the central peak, the first of the two solutions locates the X-shooter measurement near phase 0.15 ($P = 1.1697$ days) while the second locates it symmetrically about the quadrature and near phase 0.35 ($P = 1.1703$ days). Either solution is acceptable and the ambiguity does not affect the resulting orbital parameters for the DA and DQ stars. The same pattern is reproduced in the side peaks of the triplet but with a lesser significance. Table 2 lists the adopted orbital parameters. The initial epoch T_0 corresponds to the lower conjunction of the DA white dwarf. Note that the period P and the initial epoch T_0 are strongly anti-correlated.

The period and velocity amplitudes constrain the total mass of the system to $(M_{\rm DA} + M_{\rm DQ}) \sin^3 i = 1.01 \pm 0.09\, M_\odot$, where i is the inclination of the orbital plane, or $M_{\rm DA} + M_{\rm DQ} \gtrsim 0.92\, M_\odot$. The combined velocity amplitude is $K_{\rm DA} + K_{\rm DQ} = 202$ km s^{-1}. The same amplitude estimated by Vennes & Kawka (2012), $K_{\rm DA} + K_{\rm DQ} \gtrsim 320$ km s^{-1}, was in error with the correct constraint at only half of that value ($\gtrsim$160 km s^{-1}). The consequences for the merger timescale are discussed in the following section.

Figure 2 shows the radial velocity phased with the orbital period. The X-shooter data are phased by adopting one of the two possible aliases ($P = 1.1697$ days). The dispersion in Hα velocity measurements was only 10 km s^{-1} and consistent with the estimated velocity errors. The DQ velocity curve is offset by −60 km s^{-1} relative to the DA velocity curve. The effect cannot be attributed to a difference in gravitational redshifts because the mass ratio is close to unity. Instead, the pressure shift of molecular band positions is a likely cause for this effect. In the following we utilize the DA mean velocity in the calculation of the systemic velocity and Galactic kinematics.

Figure 3 shows two sets of co-added KPNO spectra, one near each quadrature. The velocity offset ($\Delta v \approx 180$ km s^{-1}) proved readily measurable.

If we adopt the spectroscopic mass estimate for the DA white dwarf based on the measured ($T_{\rm eff}$, log g) from Vennes & Kawka (2012), $M_{\rm DA} = 0.829 \pm 0.096\, M_\odot$ (following the mass–radius relations of Benvenuto & Althaus 1999) and the orbital mass ratio $q = 1.1 \pm 0.1$, then the total mass of the system is in the range 1.466–2.035 $M_\odot$. Consequently, the mass function constrains the inclination to $i = 52°$–$70°$, and the possibility of eclipses is ruled out.

3.2. Age, Evolution, and Kinematics

The cooling age of the DA white dwarf is estimated at $\tau_{\rm cool} = 1.9 \pm 0.5$ Gyr. A high mass for both white dwarfs implies relatively massive, $M_i \gtrsim 3\, M_\odot$ (see a discussion in Ferrario et al. 2005), hence short-lived progenitors (∼0.48 Gyr; Schaller et al. 1992), constraining the total age of the system to less than 3 Gyr.

Using our measured period (1.17 days) and mass ratio $q = 1.1 \pm 0.1$, and constraining the DA mass to $0.829 \pm 0.096\, M_\odot$, the merger time is estimated to be 10^{11} yr following Ritter (1986). Therefore, the system is not a candidate Type 1a supernova progenitor.

The systemic velocity was obtained by subtracting the calculated gravitational redshift ($\gamma_{\rm grav} = 54 \pm 6$ km s^{-1}) from the mean velocity of the DA white dwarf ($\gamma_{\rm DA} = 69 \pm 3$ km s^{-1}), $\gamma_{\rm sys} = \gamma_{\rm DA} - \gamma{\rm grav} = 15 \pm 7$ km s^{-1}. Adopting a distance of 40 ± 6 pc, the systemic velocity and proper-motion measurements ($\mu_\alpha \cos\delta = 2 \pm 6$, $\mu_\delta = -140 \pm 6$ mas yr^{-1}; Salim & Gould 2003) correspond to the Galactic velocity components $(U, V, W) = (0 \pm 8, -27 \pm 6, -6 \pm 2)$ km s^{-1} following Johnson & Soderblom (1987). The system belongs to the thin-disk population (Pauli et al. 2006) in agreement with its young age ($\lesssim$3 Gyr).

4. SUMMARY AND DISCUSSION

We have shown that the peculiar DQ white dwarf in NLTT 16249 is in a close 1.17 day orbit with a DA white dwarf companion. Close double-degenerate stars are common and Maxted & Marsh (1999) reported a fraction of 5%–19% of

close pairs in their radial velocity survey. White dwarfs with composite spectra indicative of DA plus DB (He I) or DA plus DC (cool He-rich) pairs are also relatively common in large surveys (see, e.g., Limoges & Bergeron 2010; Tremblay et al. 2011). However, only two DA+DQ pairs are known: NLTT 16249 and SDSS J153210.04+135615.0 (NLTT 40489) which was recently identified by Giammichele et al. (2012).

The velocity amplitudes in NLTT 16249 imply that the DQ is slightly more massive than its companion in which case it is more likely that the DQ formed first, both from $\sim 3\,M_{\odot}$ progenitors, unless stable mass transfer reversed the initial mass ratio (for detailed scenarios, see Nelemans et al. 2001). The relatively long orbital period reported here rules out the prospect of a merger within a Hubble time.

The DQ white dwarf is peculiar and the nitrogen concentration in its atmosphere is, so far, unique. Althaus et al. (2005) followed the evolution of a $2.7\,M_{\odot}$ main-sequence star past the PG1159 spectroscopic stage and down the cooling track up to the DQ stage ($0.6\,M_{\odot}$). The star follows a "born-again" He-flash loop that resets its evolution onto the post-asymptotic giant branch (post-AGB), considerably modifying the chemical structure of the outer layers that an otherwise normal post-AGB star would possess. In particular, Althaus et al. (2005) predicted measurable concentrations of nitrogen and oxygen in the atmosphere of DQ descendents of born-again stars.

The nitrogen abundance measured in the DQ component of NLTT 16249 is qualitatively similar to the abundance predicted for the 10,500 K model, the lowest temperature considered by Althaus et al. (2005). However, the C/N ratio for that particular model is close to 300, i.e., much larger than measured in NLTT 16249 ($\mathrm{C/N} \approx 50$). In the born-again context, the difference could be attributed to a different progenitor mass which could affect the outcome of the chemical evolution, although such models are not available to us. Althaus et al. (2005) also predicted a concentration of oxygen between that of carbon and nitrogen ($\mathrm{C/O} \approx 100$). It is possible to constrain the C/O abundance ratio in DQ white dwarfs using the near- and far-ultraviolet CO "Fourth-Positive" (4P) bands along with CN violet and C_2 Swan bands. Finally, the $^{13}\mathrm{C}/^{12}\mathrm{C}$ isotopic ratio expected for the same evolutionary track is well below detection limits reported by Vennes & Kawka (2012) in the case of the DQ in NLTT 16249.

What would be the role, if any, played by binary interactions in shaping the chemical structure of the DQ progenitor in NLTT 16249? The DQ white dwarfs are not known to show nitrogen in their spectra (see Dufour et al. 2005). Therefore, it may not be a coincidence that the only known detection of nitrogen in a DQ white dwarf is also that of a white dwarf in a close double-degenerate system. In that context as well, it remains to be shown that detectable traces of nitrogen would be the expected outcome of mass transfer or early envelope ejection.

S.V. and A.K. acknowledge support from the Grant Agency of the Czech Republic (GA ČR P209/10/0967, GA ČR P209/12/0217). This work was also supported by the project RVO:67985815 in the Czech Republic. We thank Donna Burton for invaluable help during the December observations at Siding Spring Observatory. J.R.T. gratefully acknowledges support from NSF grants AST-0708810 and AST-1008217.

REFERENCES

Althaus, L. G., Serenelli, A. M., Panei, J. A., et al. 2005, A&A, 435, 631
Benvenuto, O. G., & Althaus, L. G. 1999, MNRAS, 303, 30
Dopita, M., Hart, J, McGregor, P., Oates, P., & Jones, D. 2007, Ap&SS, 310, 255
Dreizler, S., & Heber, U. 1998, A&A, 334, 618
Dufour, P., Bergeron, P., & Fontaine, G. 2005, ApJ, 627, 404
Ferrario, L., Wickramasinghe, D., Liebert, J., & Williams, K. A. 2005, MNRAS, 361, 1131
Giammichele, N., Bergeron, P., & Dufour, P. 2012, ApJS, 199, 29
Johnson, D. R. H., & Soderblom, D. R. 1987, AJ, 93, 864
Koester, D., & Knist, S. 2006, A&A, 454, 951
Limoges, M.-M., & Bergeron, P. 2010, ApJ, 714, 1037
MacDonald, J., Hernanz, M., & Jose, J. 1998, MNRAS, 296, 523
Maxted, P. F. L., & Marsh, T. R. 1999, MNRAS, 307, 122
Nelemans, G., Yungelson, L. R., Portegies Zwart, S. F., & Verbunt, F. 2001, A&A, 365, 491
Pauli, E.-M., Napiwotzki, R., Heber, U., Altmann, M., & Odenkirchen, M. 2006, A&A, 447, 173
Pelletier, C., Fontaine, G., Wesemael, F., Michaud, G., & Wegner, G. 1986, ApJ, 307, 242
Ritter, H. 1986, A&A, 169, 139
Salim, S., & Gould, A. 2003, ApJ, 582, 1011
Schaller, G., Schaerer, D., Meynet, G., & Maeder, A. 1992, A&AS, 96, 269
Tremblay, P.-E., Bergeron, P., & Gianninas, A. 2011, ApJ, 730, 128
Vennes, S., & Kawka, A. 2012, ApJ, 745, L12
Werner, K., Heber, U., & Hunger, K. 1991, A&A, 244, 437
Werner, K., & Herwig, F. 2006, PASP, 118, 183